Rheological Properties of Growth-Arrested Fibroblast Cells under Serum Starvation Measured by Atomic Force Microscopy

Atsushi Miyaoka, Yusuke Mizutani, Masahiro Tsuchiya, Koichi Kawahara, and Takaharu Okajima*

Graduate School of Information Science and Technology, Hokkaido University, Sapporo 060-0814, Japan

*E-mail address: okajima@ist.hokudai.ac.jp

Abstract

The rheological properties of growth-arrested and quiescent (G0 phase) mouse fibroblast cells under serum starvation were investigated by atomic force microscopy (AFM) with a microarray technique. The number distribution of complex shear modulus, G^*, of quiescent cells at the serum concentration, $C_S = 0.1\%$, followed a log-normal distribution, and the frequency dependence of G^* exhibited a power law behavior, which were similar to those under a control condition at $C_S = 10\%$. On the other hand, we found that the Newtonian viscosity coefficient of the quiescent cells significantly increased, and the distribution broadened, as compared with the control cells, whereas the power-law exponent was unchanged. The result indicated that the rheological properties of quiescent fibroblast cells were not identical to those in the G1 phase during cell cycle. This finding suggests that the Newtonian viscosity of cells is one of the useful indicators for evaluating growth-arrested cells under serum starvation.

1. Introduction

The cell cycle is a process in which a cell duplicates into two genetically identical daughter cells and is divided into four phases, namely, G1, S, G2 and M phases. Mammalian cells dynamically change in terms of not only morphology, but also various physiological properties during the cell cycle. Therefore, it is essential to understand how cells behave in different cell phases [1)].

In order to investigate the cell cycle dependence of cell biochemical properties, some methods have been developed to synchronize cells by halting the cell cycle at a particular phase. Serum starvation, in which the concentration of serum, C_S, is lowered in cell culture, has been widely used for cells to enter the quiescent G0 phase, which is a status of growth-arrested cells having the same DNA content as that in the G1 phase [1-4)]. It is known that quiescent cells can reenter the cell cycle through the restriction point in the late G1 phase when transferred into a medium with a relatively high C_S [1-4)].

Since an organism mostly consists of G0 cells with a small number of stem cells, understanding the biochemical properties of G0 cells helps us to comprehend the organization of tissues and the organism. Previous studies [5, 6)] revealed that fission yeast cells, which are a eukaryotic model, remained metabolically active in the G0 phase, but differed markedly from cycling cells in the G1 phase in heat resistance, cytoplasmic and nuclear morphologies, as well as proteolysis and protein synthesis.

The importance of investigating the mechanical and viscoelastic properties of living cells at a single cell level is increasingly being recognized as an approach to understanding cell behavior [7)]. Atomic force microscopy (AFM) has been employed to

conduct direct mechanical measurements of single cells in the M phase [8-10] and G1 phase [11]. Moreover, the cell cycle dependence of adhesion forces was investigated by force spectroscopy [12]. However, as far as we know, no experiment regarding the viscoelastic properties of cell cycle-arrested single cells has been reported, and thus it is unknown how a method to arrest cell phase influences cell rheology. One reason for the lack of such experiments may be due to the difficulty of statistical estimation of cell cycle-arrested cells with their inherent individual differences.

The aim of this study was to investigate how cell rheology is affected by serum starvation, with an AFM method that allows us to measure the number distribution of the rheological properties of cells [13, 14]. In the AFM method, the cells were arranged and cultured in a microfabricated glass substrate so that the AFM force measurements of many different cells were performed automatically. We found that the number distribution of complex shear modulus G^* of the quiescent G0 cells followed a log-normal distribution and a single power law behavior [14-24] as a function of frequency. Interestingly, the number distribution of the Newtonian viscosity coefficient of cells broadened, as compared with that under a control condition. The value of the former was obviously larger than that of the latter although the exponent of power-law rheology was almost unchanged. This indicated that the rheological properties of fibroblast cells in the quiescent G0 phase were different from those in the G1 phase during cell cycle.

2. Materials and Methods

2.1 Microarray

A commercial cell microarray (Nunc LiveCell Array), which had a hexagonal structure of microwells with a depth of ~8 μm and a spacing of 20 μm on a glass substrate, was used as a culture substrate. The substrate was precoated with fibronectin (BD Bioscience).

2*.2 Cell samples*

Mouse fibroblast NIH3T3 cells were cultured at 37 °C and 5% CO_2 atmosphere in Dulbecco's modified Eagle's medium DMEM (Sigma) containing penicillin (100 units/mL), streptomycin (100 mg/mL) (Sigma), and fetal bovine serum (FBS; HyClone) at C_S = 0-10%. The DNA content of cells under serum starvation was estimated using a flow cytometer (Becton Dickinson FACSCanto II) with software (TreeStar FlowJo).

After NIH3T3 cells were cultured for 24 h in the medium with C_S = 0.1 and 10%, they were suspended with trypsin-EDTA (Sigma), deposited on the microarray in complete medium (DMEM containing FBS), and immediately incubated for ~ 24 h under the same medium conditions [Fig. 1(a)]. The cells were washed with CO_2-independent medium (GIBCO), placed in the same medium and immediately used for AFM experiments. We have confirmed that the cells are arranged in the wells of the microarray and that the filling rate of cells to wells is > 98% from a fluorescence image of the nuclei in a large scale [13].

2.3 Force modulation measurements

We used a commercial AFM (Asylum Research MFP-3D AFM) mounted in an inverted optical microscope (Nikon TE-2000E). A colloidal silica bead with a radius of ~3 μm (Funakoshi) was attached to the tip apex of the cantilever (Olympus BL-AC40TS) using an epoxy glue [13, 14, 25]. The spring constant was determined using a built-in thermal fluctuation method. The loading force was determined on the basis of Hooke's law by multiplying the calibrated cantilever spring constant by its deflection.

The AFM measurements were examined at the centers of the wells [Fig. 1(b)]. A maximum loading force of ~ 500 pN was applied to the cell surface for ca. 30 s, and a reference signal of sinusoidal oscillation with an amplitude of 10 nm and frequency, f, in the range of 2-100 Hz was added to the z piezo of AFM to move the cantilever vertically. The amplitude and phase shift of the cantilever displacement with respect to the reference signal were measured using an external digital lock-in amplifier (SEIKO EG&G, 7260) with a time constant of ~0.5 s.

The loading force F^*, which is complex as indicated by the asterisk, with the small oscillating indentation, δ_1^*, around an operating indentation, δ_0 was approximately expressed [26-28], using a Hertz model, by

$$F^* = \frac{4R^{1/2}}{3\left(1-\nu^2\right)}\left(E_0{\delta_0}^{3/2} + \frac{3}{2}{E_1}^*{\delta_0}^{1/2}{\delta_1}^*\right), \qquad (1)$$

where ν is the Poisson's ratio of the cell, R is the radius of the spherical probe, and E_0 is the elastic modulus at zero frequency obtained from the slow approach force curve. E_1^* is the frequency-dependent elastic modulus to be $2(1+\nu)G^*$ [29]. The value of ν was assumed to be 0.5 [14, 30].

The probe moving through the surrounding liquid experiences not only the force applied to the cell but also the hydrodynamic drag force F_d^* [31]. Thus, G^* of cells is given [22] by

$$G^* = G' + iG'' = \frac{1-\nu}{4(R\delta_0)^{1/2}}\left[\frac{F_1^*}{\delta_1^*} - ib(0)f\right], \qquad (2)$$

where $F_1^* = 2(R\delta_0)^{1/2} E_1^* \delta_1^* / (1-\nu^2)$, and b is the so-called drag factor [31], in which F_d^* at a separation distance, h, between the cell surface and the probe with the oscillation amplitude δ_1^* is defined as $F_d^*/\delta_1^* = ib(h)f$. The $b(0)$ was determined from the extrapolation of $b(h)$ measured at f = 100 Hz. The phase shift of the AFM instrument at different frequencies was calibrated using a stiff cantilever in contact with a clean glass cover slip in air.

3. Results and Discussion

Figure 2(a) shows the ratios of G0/G1, S/G2, and M phases in the NIH3T3 cells at different C_S values, measured using the flow cytometer. As C_S decreased, the ratio of cells in the G0/G1 phase was gradually increased after an incubation time of 24 h and reached a maximum of about 90% at around C_S = 0.1% after 48 h. This result indicated that the cells could be highly growth-arrested at C_S = 0.1%. Moreover, as shown in Fig. 2(b), cell proliferation rate drastically decreased with decreasing C_S and the proliferation almost halted at less than Cs = 0.1%. The decrease in cell count after 48 h at C_S = 0.1 or 0% was probably due to cell death. Figure 2(c) shows the distribution of DNA content of cells that were serum-starved at C_S = 0.1% for 48 h and then transferred

to a medium with C_S = 10% at t =0 s. The enhancement of the peak indicated by the arrow showed the increase in the number of cells that duplicated DNA and changed from G0/G1 to other phases, indicating that the cells growth-arrested at C_S = 0.1% could reenter cell cycle.

Figure 3 shows the distribution of storage *G'* and loss *G"* moduli of cells cultured in the wells of the microarray with a medium at C_S= 0.1% (the number of cells, n=120) measured by AFM at different frequencies. The distributions were log-normal, and the peak of the distribution increased with increasing frequency. It seemed that the variation of the distribution of *G"* became narrower than that of *G'* in the frequency range of 2−100 Hz. Such features of distributions have been reported recently [14)], although the origin of the features has not been elucidated.

Figures 4 (a) and 4(b) show the average *G'* and *G"* of the NIH3T3 cells at C_S = 10 (n = 70) and 0.1% (n = 120), respectively, as a function of frequency in the range of 2−100 Hz. The *G'* of the cells increased linearly in a log-log scale, exhibiting a weak power-law dependence of *G'* on oscillation frequency. On the other hand, *G"* was approximately threefold lower than *G'* and displayed a similar frequency dependence on *G'* at low frequencies < ~10 Hz, and the frequency dependence became more pronounced at higher frequencies. Such a behavior of the power-law frequency dependence has been observed in several cell types [14-24)]. The data shown in Fig. 4 was well fitted to the power-law structural damping model [15, 16, 32, 33)] with additional Newtonian viscosity, which is expressed by

$$G^* = G_0(1+i\eta)\left(\frac{f}{f_0}\right)^{\alpha}\Gamma(1-\alpha)\cos\left(\frac{\pi\alpha}{2}\right)+i\mu f\,, \qquad (3)$$

where α is the power-law exponent of the model. η is the hysteresivity, which is expressed by $\tan(\pi\alpha/2)$. G_0 is a modulus scale factor, f_0 is a frequency scale factor, Γ denotes the gamma function, and μ is the Newtonian viscosity coefficient.

Figure 5 shows the distributions of α and μ of NIH3T3 cells measured by AFM. The α is one for solid like behavior and zero for fluid-like behavior. The distribution of α at both C_S = 10 and 0.1% was normal Gaussian rather than log-normal. The average α values were 0.22 at C_S = 10% and 0.18 at C_S = 0.1%, and no significant difference was found between them.

On the other hand, as shown in Fig. 5, we found that the distribution of μ at C_S = 0.1% became much broadened compared with that at C_S = 10%, although these distributions were not completely separated. Namely, μ at C_S = 0.1% was widely distributed in the range of 0 - 2.0 Pa·s, while most of μ' s at C_S = 10% was less than 1.0 Pa·s. The results indicated that cells that growth-arrested under serum starvation were not identical to those in the phases during cell cycle, but had a specific feature, which is different from that in the G1 phase, from the rheological point of view. μ is mainly related to interactions between actin filaments and the surrounding materials as well as among other cytoplasmic materials. Therefore, the result shown in Fig. 5(b) implies that the components and quantities of proteins in cells are largely varied under serum starvation.

It was revealed that fission yeast cells in the G0 phase were metabolically active, but differed from cycling cells in the G1 phase in physiological response such as heat resistance and also in cytoplasmic and nuclear morphologies.[5)] Moreover, recently, it has been reported [6)] that proteolysis was required for maintaining G0 quiescence of fission yeast cells under nitrogen-starved condition, and protein synthesis and the autophagy-mediated destruction of mitochondria occurred in the G0 cells. The results suggest that the concentration and the components of proteins in cytoplasmic regions of cells in the G0 phase largely vary from those of cycling cells in the G1 phase. The proteolysis and protein synthesis in the cytoplasm may cause the increase in μ observed in growth-arrested cells under serum starvation.

The AFM allows us to measure rheological properties of cells not only in the frequency domain, but also in the time domain.[34-38)] Time domain AFM is relatively simple to measure the rheological properties of cells, compared with the frequency domain, but physical (rheological) quantity cannot be directly determined from the observed parameters by time domain AFM, without any rheology model.[39)] The rheological property of cell that μ changes without any obvious change in α can be utilized as a model for time domain AFM to evaluate cells that are cell cycle-arrested under serum starvation.

4. Conclusions

We succeeded in measuring the number distribution of the complex shear modulus of NIH3T3 cells growth-arrested under serum starvation by AFM with a cell microarray. It

was found that the distribution of the Newtonian viscosity coefficient was markedly different between quiescent and control cells, while other parameters were not significantly changed. This result indicated that the rheological properties of cells growth-arrested under serum starvation had a specific feature that is different from G1 phase. Therefore, the measurement of the Newtonian viscosity of cells is crucial to evaluate cells growth-arrested under serum starvation.

Acknowledgments

We would like to thank Dr. Yusuke Toyoda for his fruitful comments. This work was supported by the Industrial Technology Research Grant Program (2006) from the New Energy and Industrial Technology Development Organization (NEDO) of Japan, a Grant-in-Aid for Scientific Research B (No. 21310079), a Grant-in-Aid for Scientific Research on Priority Areas “Molecular Science for Supra Functional Systems” (No. 19056009) and the Global-COE Program “Center for Next-Generation Information Technology based on Knowledge Discovery and Knowledge Federation” from the Ministry of Education, Culture, Sports, Science and Technology of Japan.

References

1) B. Alberts, A. Johnson, J. Lewis, M. Raff, K. Roberts, and P. Walter: *Molecular Biology of the Cell* (Garland Science, 2008) 5th ed., Chap. 17.

2) A. Zetterberg and O. Larsson: Proc. Natl. Acad. Sci. U.S.A. **82** (1985) 5365.

3) R. D. Woessner, M. R. Mattern, C. K. Mirabelli, R. K. Johnson, and F. H. Drake: Cell Growth Differ. **2** (1991) 209.

4) S. Cooper: FASEB J. **17** (2003) 333.

5) S.S. Su, Y. Tanaka, I. Samejima, K. Tanaka, and M. Yanagida: J. Cell Sci. **109** (1996) 1347.

6) K. Takeda, T. Yoshida, S. Kikuchi, K. Nagao, A. Kokubu, T. Pluskal, A. Villar-Briones, T. Nakamura, and M. Yanagida: Proc. Natl. Acad. Sci. U.S.A. **107** (2010) 3540.

7) D. E. Ingber: J. Cell Sci. **116** (2003) 1157.

8) R. Matzke, K. Jacobison, and M. Radmacher: Nat. Cell Biol. **3** (2001) 607.

9) P. Kunda, A. E. Pelling, T. Liu, and B. Baum: Curr. Biol. **18** (2008) 91.

10) M. P. Stewart, J. Helenius, Y. Toyoda, S. P. Ramanathan, D. J. Müller, and A. A. Hyman: Nature **469** (2011) 226.

11) P. Roca-Cusachs, J. Alcaraz, R. Sunyer, J. Samitier, R. Farré, and D. Navajas: Biophys. J. **94** (2008) 4984.

12) G. Weder, J. Vörös, M. Giazzon, N. Matthey, H. Heinzelmann, and M. Liley: Biointerphases **4** (2009)27.

13) Y. Mizutani, M. Tsuchiya, S. Hiratsuka, K. Kawahara, H. Tokumoto, and T.

Okajima: Jpn. J. Appl. Phys. **47** (2008) 6177.

14) S. Hiratsuka, Y. Mizutani, M. Tsuchiya, K. Kawahara, H. Tokumoto, and T. Okajima: Ultramicroscopy **109** (2009) 937.

15) B. Fabry, G. N. Maksym, J. P. Butler, M. Glogauer, D. Navajas, and J. J. Fredberg: Phys. Rev. Lett. **87** (2001) 148102

16) B. Fabry, G. N. Maksym, J. P. Butler, M. Glogauer, D. Navajas, N. A. Taback, E. J. Millet, and J. J. Fredberg: Phys. Rev. E **68** (2003) 041914.

17) L. Deng, X. Trepat, J.P. Butler, E. Millet, K. G. Morgan, D. A. Weitz, J. J. Fredberg: Nat. Mater. **5** (2006) 636.

18) B. D. Hoffman, G. Massiera, K. M. Van Citters, and J. C. Crocker: Proc. Natl. Acad. Sci. U.S.A. **103** (2006) 10259.

19) K. M. Van Citters, B. D. Hoffman, G. Massiera, and J. C. Crocker: Biophys. J. **91** (2006) 3946.

20) G. Massiera, K. M. Van Citters, P. L. Biancaniello, and J. C. Crocker: Biophys. J. **93** (2007) 3703.

21) M. Balland, N. Desprat, D. Icard, S. Féréol, A. Asnacios, J. Browaeys, S. Hénon, and F. Gallet: Phys. Rev. E **74** (2006) 021911.

22) J. Alcaraz, L. Buscemi, M. Grabulosa, X. Trepat, B. Fabry, R. Farre, and D. Navajas: Biophys. J. **84** (2003) 2071.

23) B. A. Smith, B. Tolloczko, J. G. Martin, and P. Grütter: Biophys. J. **88** (2005) 2994.

24) P. Roca-Cusachs, I. Almendros, R. Sunyer, N. Gavara, R. Farre, and D. Navajas: Biophys. J. **91**(2006) 3508.

25) T. Okajima, M. Tanaka, S. Tsukiyama, T. Kadowaki, S. Yamamoto, M. Shimomura, and H. Tokumoto: Jpn. J. Appl. Phys. **46** (2007) 5552.

26) M. Radmacher, R. W. Tillmann, M. Fritz, and H. E. Gaub: Science **257** (1992) 1900.

27) M. Radmacher, R. W. Tillmann, and H. E. Gaub: Biophys. J. **64** (1993) 735.

28) R. E. Mahaffy. S. Park, E. Gerde, J. Käs, and C. K. Shih: Biophys. J. **86** (2004) 1777.

29) L. D. Landau and E. M. Lifshiz: *Theory of Elasticity* (Pergamon Press, Oxford, U.K., 1986).

30) *Methods in Cell Biology, Atomic force microscopy in cell biology*, ed. B. P. Jena and J. K. H. Hörber (Academic Press, USA, 2002) vol. 68.

31) J. Alcaraz, L. Buscemi, M. Puig-De-Morales, J. Colchero, A. Baro, and D. Navajas: Langmuir **18** (2002) 716.

32) J. J. Fredberg and D. Stamenovic: J. Appl. Physiol. **67** (1989) 2408.

33) J. Hildebrandt: Bull. Math. Biophys. **31** (1969) 651.

34) H. W. Wu, T. Kuhn, and V. T. Moy: Scanning **20** (1998) 389.

35) E. M. Darling, S. Zauscher, and F. Guilak: Osteoarthr. Cartilage **14** (2006) 571.

36) E. M. Darling, S. Zauscher, J. A. Block, and F. Guilak: Biophys. J. **92** (2007) 1784.

37) T. Okajima, M. Tanaka, S. Tsukiyama, T. Kadowaki, S. Yamamoto, M. Shimomura, and H. Tokumoto: Nanotechnology **18** (2007) 084010.

38) S. Hiratsuka, Y. Mizutani, A. Toda, N. Fukushima, K. Kawahara, H. Tokumoto, and T. Okajima: Jpn. J. Appl. Phys. **48** (2009) 08JB17.

39) W. N. Findley, J. S. Lai, and K. Onaran: *Creep and Relaxation of Nonlinear Viscoelastic Materials with an Introduction to Linear Viscoelasticity* (Dover, New York, 1989).

Figure captions

Fig. 1. (a) After NIH3T3 cells were cultured for 24 h at different serum concentrations (C_S = 0.1 or 10%) in dishes, the cells were placed on microarray and cultured for ~24 h at the same serum concentration. The phase of cells was estimated by measuring the DNA content of cells (green, G0/G1; yellow-green, S/G2; blue, M phase) using flow cytometer. (b) Schematic diagram of AFM combined with a microarray substrate, on which living cells were placed. The force modulation mode measurements were conducted at the center of the wells of the microarray in CO_2-independent medium with the same serum concentration.

Fig. 2 (a) Ratios of NIH3T3 cells in various phases incubated for 24 h (filled) and 48 h (open) at different C_S's, measured with the flow cytometer. The red, green, and blue columns represent the G0/G1, S/G2, and M phases, respectively. (b) Proliferation of cells incubated for 0 h (filled), 24 h (dotted), and 48 h (open) at different C_S's. (c) Distribution of DNA content of cells cultured for 48 h at C_S = 0.1% and then transferred to a medium at C_S = 10%. The arrow represents cells that duplicated DNA.

Fig. 3 Distributions of storage *G*' (left) and loss *G*'' (right) moduli of NIH3T3 cells growth-arrested under serum starvation in the wells of the microarray. The plot is presented using a logarithmic scale at different frequencies of (a) 5, (b) 25, and (c) 100 Hz.

Fig. 4 Average *G*' (open) and *G*'' (filled) of NIH3T3 cells in the wells of the microarray at C_S = 10 (a) and 0.1% (b) as a function of frequency. The symbols represent the geometric mean. Solid lines represent the resultant fit of the power-law structural damping model described by eq. (3).

Fig. 5 Distributions of power-law exponent α and Newtonian viscosity coefficient μ of NIH3T3 cells, estimated using eq. (3), at C_S = 10 (left) and 0.1% (right). Solid lines represent a normal Gaussian fit.

Fig.1 Miyaoka et al.

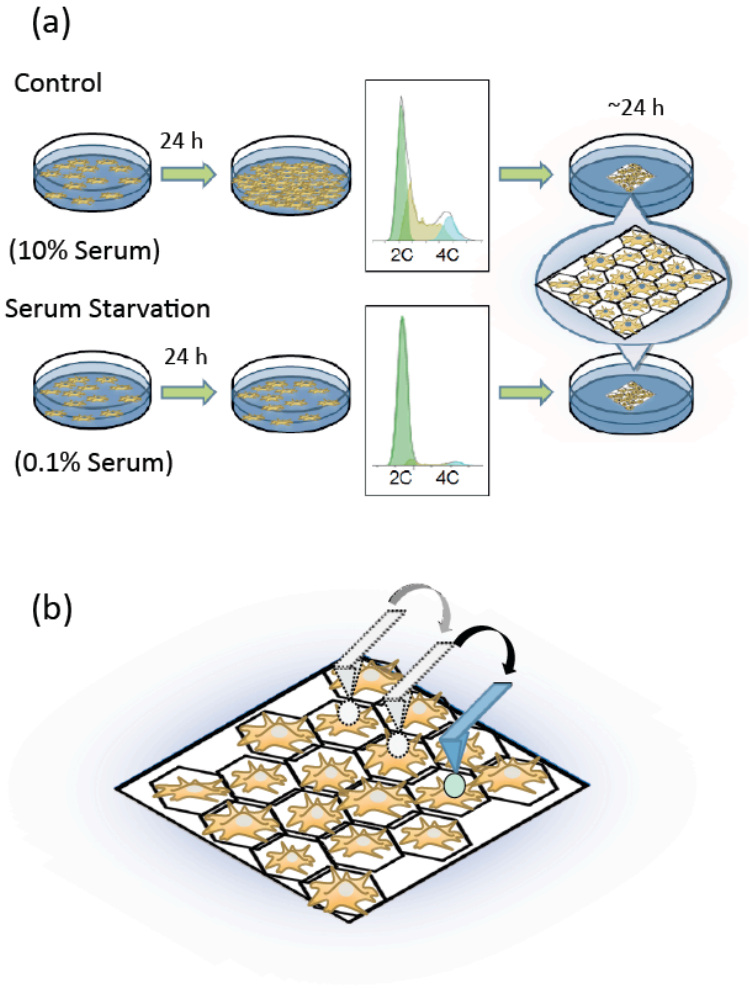

Fig.2 Miyaoka et al.

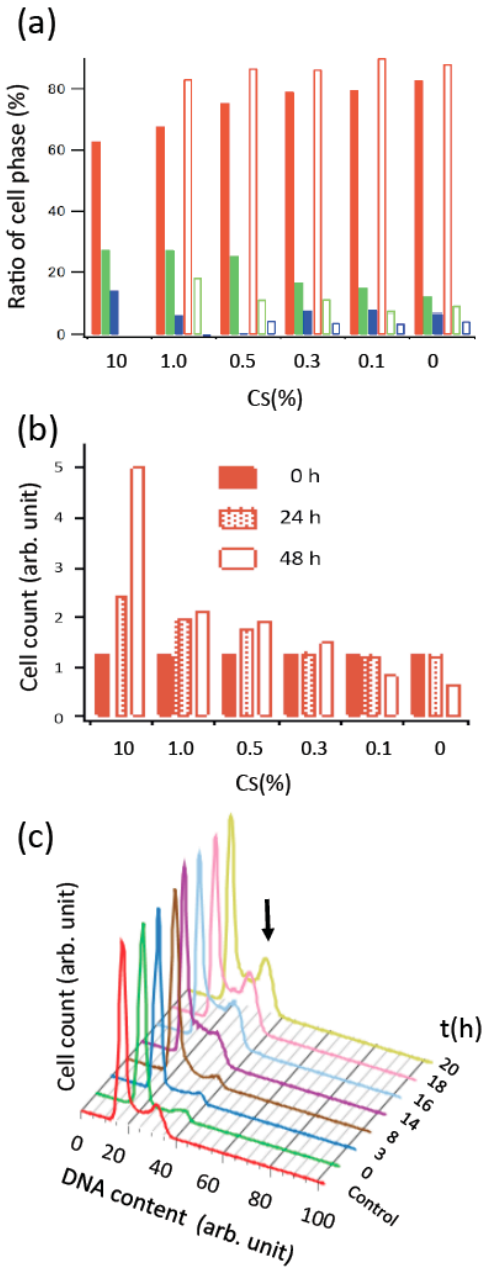

Fig.3 Miyaoka et al.

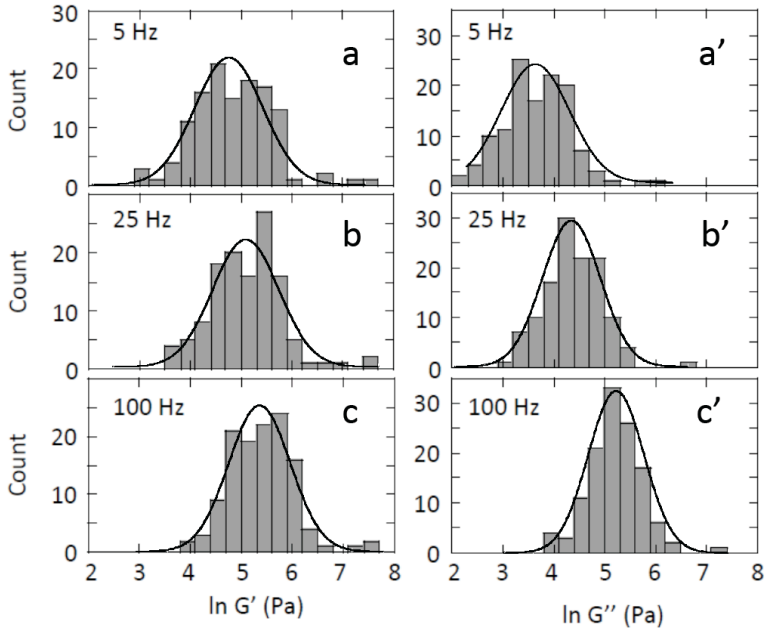

Fig.4 Miyaoka et al.

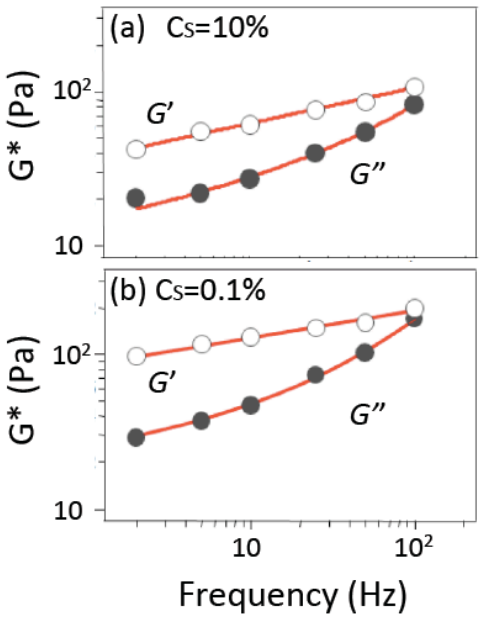

Fig.5 Miyaoka et al.